Int J Nutr Sci 2026;11(3):1-9

International Journal of Nutrition Sciences

Journal Home Page: ijns.sums.ac.ir

ORIGINAL ARTICLE

In Vitro Effect of Folic Acid-Targeted, pH-Responsive and Superparamagnetic Iron Oxide Nanoparticles for Selective Camptothecin Delivery to Prostate Cancer Cells

Musaab Mohammed Kadhim[1*], Qasim Najim Thewaini[1], Sharafaldin Al-Musawi[2]

1. Biotechnology Medical Department, College of Biotechnology, Al-Qasim Green University, Babylon, Iraq
2. Food Science Department, College of Food Science, Al-Qasim Green University, Babylon, Iraq

ARTICLE INFO

Keywords:
Folic Acid
Superparamagnetic iron oxide nanoparticles
Camptothecin
Prostate cancer

**Corresponding author:*
Musaab Mohammed Kadhim, MSc;
Biotechnology Medical Department,
College of Biotechnology,
Al-Qasim Green University,
Babylon, Iraq.
Tel: +964 7725801071
Email: musd97073@gmail.com
Received: April 1, 2026
Revised: June 25, 2026
Accepted: July 1, 2026

ABSTRACT

Background: Developing targeted drug delivery; while reducing toxicity is undertaken to enhance therapeutic efficacy. This study focused on engineering a nanocomposite used to selectively deliver camptothecin (CPT), an effective anticancer drug, to prostate cancer cells via folic acid receptors.

Methods: Nanocomposite, composed of supermagnetic iron oxide-dextran-camptothecin-folic acid nanoparticles (SPION-DEX-CPT-FA), was synthesized by co-precipitation. The nanocomposites were characterized using dynamic light scattering (DLS), transmission and scanning electron microscopy, vibrating sample magnetometry (VSM), and Fourier transform infrared spectroscopy (FTIR). Drug encapsulation, pH-responsive release kinetics, cellular uptake, selective cytotoxicity (MTT assay), and apoptosis (by flowcytometry) were performed to evaluate the *in vitro* effect on prostate cancer cells and prostate normal cells.

Results: The synthesized nanocomposite had an average spherical diameter of 64.38 nm and a strong negative zeta potential of -43.8 mV. With a magnetic strength of 58 emu/g FTIR analysis, the successful coupling of all components was confirmed. The nanocomposite exhibited superior magnetic properties. It also demonstrated a very high drug encapsulation efficiency. The system exhibited a pH-stimulated release pattern, with accelerated CPT release at an acidic pH (5.4) compared to physiological pH (7.4). An enhanced uptake was verifie by prostate cancer cells. The formulation demonstrated strong cytotoxicity and discrimination against cancer cells (IC50=12 µg/ml at 24 h).

Conclusion: SPION-DEX-CPT-FA nanocomposite represented a promising platform for drug delivery. Its targeted delivery, precise release, selective anticancer activity suggest its potential use as an effective treatment for prostate cancer.

Please cite this article as: Kadhim MM, Thewaini QN, MAl-Musawi S. In Vitro Effect of Folic Acid-Targeted, pH-Responsive and Superparamagnetic Iron Oxide Nanoparticles for Selective Camptothecin Delivery to Prostate Cancer Cells . Int J Nutr Sci. 2026;11(3):1-9.

Introduction

Prostate cancer remains a significant global health challenge, also a leading cause of cancer-related mortality in men (1). Conventional treatment, as well as chemotherapy, radiation, and androgen-deprivation therapy (ADT), are frequently hampered by extensive limitations such as systemic toxicity, deficiency of specificity, the development of medicine resistance (2). Traditional chemotherapeutic representatives indiscriminately affect both malevolent and healthy rapidly dividing cells, leading to severe side effects that weaken the patient's quality of life and narrow the therapeutic window. These challenges underscore the vital need for innovative therapeutic strategies that can precisely target cancer cells while carefully preserving healthy tissue (3-5).

Nanomedicine has developed as a transformative approach to statement the shortcomings of conventional cancer therapy. Nanomaterials can also be used to treat bacterial infections of the urinary tract (6). Nanoparticle-based drug delivery systems (DDS) have the potential to revolutionize behavior by improving the pharmacokinetic properties of drugs, protecting them from premature degradation, and enhancing their uptake at the tumor site (6). This can be achieved through equally passive targeting, which leverages the greater permeability and retention effect of tumor vasculature, and active targeting, which involves functionalizing the nanoparticle's external surface with ligands that bind to specific receptors overexpressed on cancer cells. Such besieged strategies promise to maximize therapeutic efficacy while minimizing off-target toxicity (7-9).

Camptothecin (CPT) as a multifunctional nanocomposite has been utilized for the targeted delivery and is considered a potent topoisomerase inhibitor through its broad-spectrum anticancer activity (10). The clinical utility of CPT is severely limited by way of its poor aqueous solubility, predictability of its active lactone ring at physiological pH, and frequent addition of significant side effects. Encapsulating CPT into nanocarriers can overcome these challenges by its solubility, stability and bioavailability (11-13). A core of superparamagnetic iron oxide nanoparticles (SPIONs), which are biocompatible too offer theranostic potential have been designed for magnetic resonance imaging (MRI) and magnetic hyperthermia (14-16).

To achieve biocompatibility and energetic targeting, the SPION central is coated with dextran, a biodegradable polysaccharide that enhances stability and offers a matrix for drug loading, and functionalized through folic acid (FA) (17). Folic acid serves as an aiming ligand for the folate receptor (FR), which is frequently overexpressed on the surface of several cancer cells, including prostate cancer, but requires limited expression in normal tissues. This approach aims to activate receptor-mediated endocytosis for the discriminating internalization of the nanocomposite added to cancer cells, thereby concentrating the therapeutic freight where it is most needed (18, 19). The principal objective of this research was to synthesize and comprehensively distinguish the supermagnetic iron oxide-dextran-camptothecin-folic acid nanoparticles (SPION-DEX-CPT-FA) platform and to evaluate its potential for targeted, pH-responsive drug delivery, as well as selective cytotoxicity against prostate cancer cells *in vitro* (20). Also, SPION@DEX-CPT-FA SPION was synthesized by the co-precipitation method to control cancer cells using CPT and the biodegradable dextran (DEX) under acidic conditions.

Materials and Methods

SPIONs served as the core material; whilet the SPION@DEX-CPT-FA nanocomposite was synthesized using a co-precipitation method. First, 50 mg of DEX powder was dissolved in 1 mL of a 1% (w/v) acetic acid solution containing the SPION suspension. Subsequently, 10 mg of CPT was mixed with the Dex-iron oxide solution. This mixture was added dropwise into 50 mL of double-distilled water (DDW) preserved at 60°C. Concurrently, 1 mL of a 20% (w/w) sodium citrate solution was gently introduced to maintain a neutral pH, and the feedback proceeded for an additional 20 minutes. The resultant nanoparticles were separated with a strong external magnet, washed multiple times with isopropanol, and dried overnight at 65°C. To end, the nanocomposite stayed functionalized by incorporating 5 mg/mL of FA added to the mixture. A drug-free construction (SPION-DEX) was also prepared using the matching protocol for comparative purposes. Dynamic Light Scattering (DLS) analysis was utilized to discover the iron oxide (Fe_3O_4) nanoparticles.

The dynamic diameter and zeta potential of the nanocomposite were determined using a Zeta-Sizer. The sample was organized by dispersing 1 mg/mL of the nanocomposite in double-distilled water, in addition to sonicating for 15 seconds in an ice bath. The internal morphology was assessed using transmission electron microscopy (TEM) at 120 kV. A diluted solution of the nanoformulation was deposited against a carbon-coated copper net for imaging. The surface morphology was assessed using scanning electron microscopy (SEM). The dry sample was fixed to aluminum tips, coated with a gold-palladium layer, and imaged at an accelerating voltage of 25 kV. The magnetic appearances of the

nanoparticles were evaluated using a Vibrating Sample Magnetometer (VSM) to regulate the magnetization of the sample when exposed to an external magnetic field. Fourier Transform Infrared (FTIR) spectra confirmed the chemical composition and positive conjugation. Samples such as potassium bromide (KBr) pellets were prepared, and spectra were found in the range of 400–4000 cm−1.

The amount of CPT encapsulated surrounded by the nanocomposite was quantified. The formulation was distributed in DDW, sonicated, and then centrifuged at 14,000 rpm. The concentration of unencapsulated CPT in the supernatant was measured using fluorescence spectroscopy. Encapsulation efficiency (EE%) was considered using the formula of EE%=((Total quantity of drug- ree quantity of drug)/Total amount of drug)×100. The release of CPT was investigated at 37°C in two different buffer solutions: phosphate buffer solution (PBS) at pH 7.4, in addition to citrate buffer solution (CBS) at pH 5.4. One milliliter of the nanodrug solution was placed in a dialysis bag and immersed in 100 mL of the respective cushion solution, with samples taken finished 96 hours.

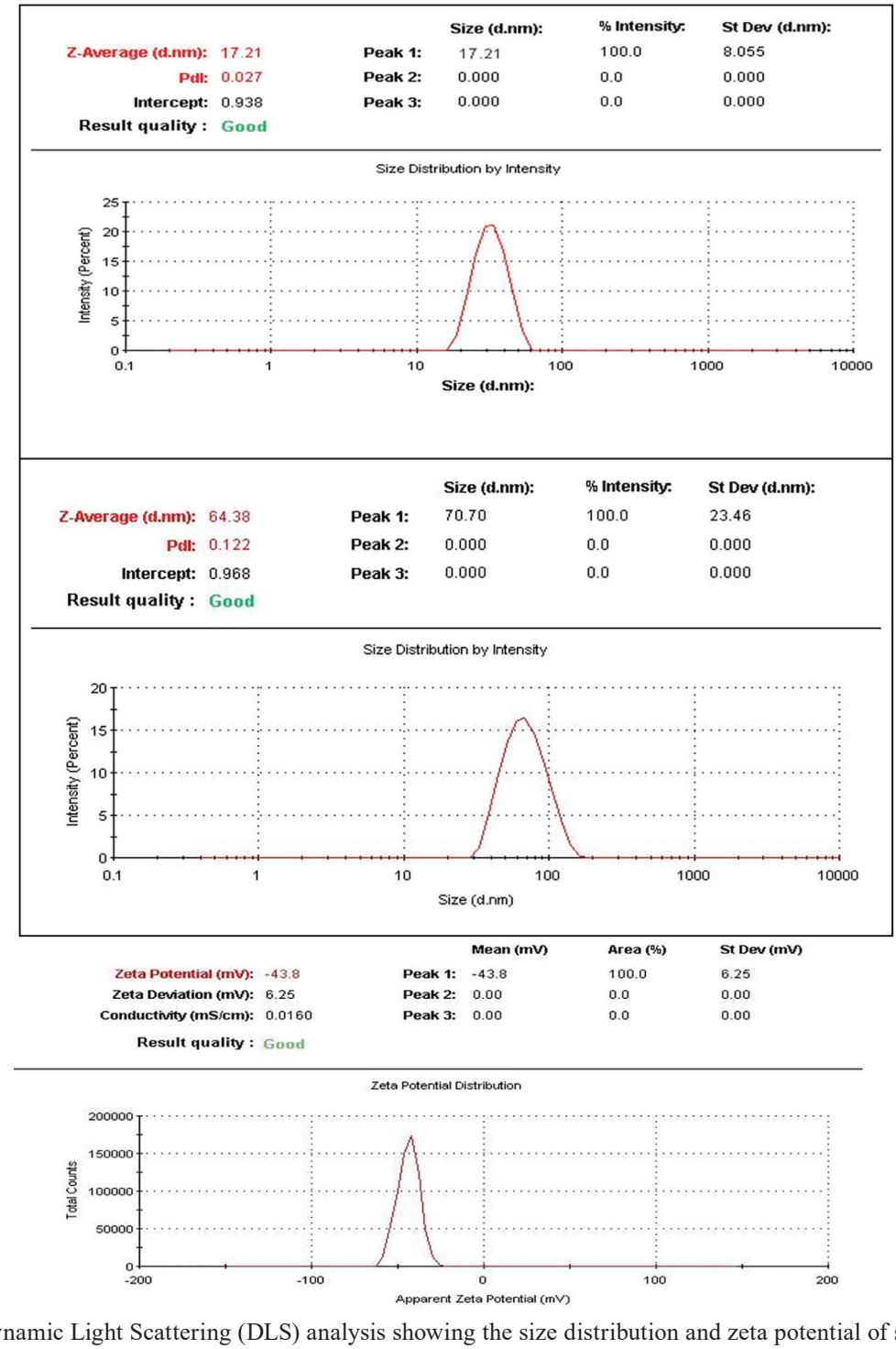

Figure 1: Dynamic Light Scattering (DLS) analysis showing the size distribution and zeta potential of supermagnetic iron oxide-dextran-camptothecin-folic acid nanoparticles (SPION-DEX-CPT-FA).

The normal prostate cell line (BPH-1) and the prostate cancer cell line (PC-310) were cultured, respectively, in Dulbecco's Modified Eagle Medium (DMEM). The DMEM medium, maintained at 37°C in a humidified environment with 5% CO_2, contained 1% penicillin and streptomycin, 10% fetal bovine serum, and 200 mM glutamine . To visualize cellular uptake, the nanocomposite was considered with fluorescein isothiocyanate (FITC). Prostate cancer cells were protected with the FITC-labeled nanoparticles and imaged with a fluorescence microscope to observe internalization. The cytotoxic effect of the formulations was evaluated on both prostate cancer cells and prostate normal cells using the MTT assay. Cells were frozen with various concentrations of free CPT, empty nanoparticles, in addition to CPT-loaded nanoparticles for 24 to 48 hours. Cell viability was assessed based on mitochondrial activity.

Flow cytometry was used to quantify the extent of apoptosis. Prostate cancer cells were treated with the constructions for 48 hours, stained, and analyzed in the direction to determine the percentage of cells suffering from apoptosis. Statistical analyses were carried out by SPSS software (Version 22, Chicago, IL, USA) and data were processed using unpaired student's t-test and ANOVA. Data were expressed as standard fault of the mean (mean±SEM), with*p<0.05 considered as statistically significant. Three replicates were made in for each assay (21).

Results

(DLS analysis could discover that the naked Fe_3O_4 nanoparticles exhibited a narrow size distribution with an average hydrodynamic thickness of 17.21 nm. Following surface change and drug loading, the final FA-DEX-CPT-SPION nanocomposite showed a significant growth in average particle size to 64.38 nm. The zeta potential of the final SPION@DEX-CPT-FA formulation was measured at –43.8 mV as indicated in Figure 1. SEM and TEM were conducted to perceive the morphology of the nanoparticles (Figure 2-a and 2-b). The images illustrate that both the naked Fe_3O_4 nanoparticles, in addition to the final SPION@DEX-CPT-FA nanocomposite, were spherical in shape and exhibited an even size distribution (Figure 2a, and 2b).

The VSM results showed that the naked SPIONs had a saturation magnetization value of 21emu/g. After surface modification, the SPION@DEX-CPT-FA nanocomposite showed a reduced saturation magnetization of 58 emu/g. The VSM curves for both

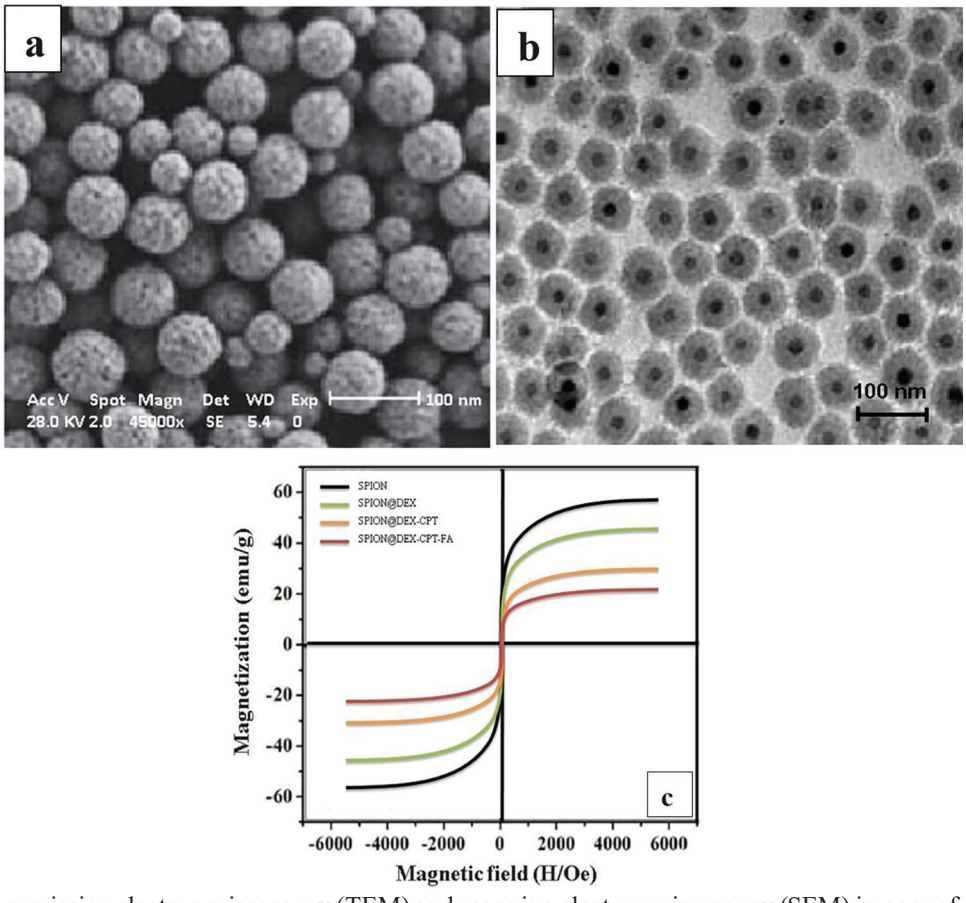

Figure 2: a. transmission electron microscopy (TEM) and scanning electron microscopy (SEM) images of supermagnetic iron oxide nanoparticles (SPIONs). b. supermagnetic iron oxide-dextran-camptothecin-folic acid nanoparticles (SPION-DEX-CPT-FA) nanoparticles showing spherical morphology and coating structure. c. Magnetization curves of uncoated SPIONs and SPION@DEX-CPT-FA obtained by VSM, showing superparamagnetic behavior.

samples showed no hysteresis or coercivity, which is characteristic of superparamagnetic behavior (Figure 2-c).

FTIR spectra confirmed the chemical structure at synthesis stage. The spectrum for nude SPIONs (a) showed a characteristic Fe–O vibration highest at 592 cm−1. For dextran-coated SPIONs (b), original peaks corresponding to the etheric bond (1030 cm−1) and –CH2– stretching (2923 cm−1) of dextran gave the impression. The spectrum for SPION-DEX-CPT (c) revealed peaks for amine groups (1278, 3285, and 3198 cm−1) from CPT. The final spectrum of SPION-DEX-CPT-FA (d) showed a distinct new peak at 1688 cm−1, corresponding to the carboxyl group of folic acid (Figure 3). The encapsulation efficiency (EE%) of CPT in the SPION@DEX-CPT-FA nano formulation was calculated to be 64.38%. This was significantly higher than the EE% in nude SPIONs, which was 17.21%. The *in vitro* medicine release profile was studied completed 96 hours at pH 7.4 and pH 5.4. The results displayed that CPT release was slower at the physiological pH of 7.4, while a quicker and more sustained release pattern was experimental at the acidic pH of 5.4 (Figure 3).

Fluorescence microscopy was used to visualize the uptake of the nanocomposite by prostate cancer cells (4a). Cells treated with FITC-labeled SPION@ DEX-CPT-FA (Figure 4-b) displayed a strong green fluorescence signal within the cytoplasm Figure (Figure 4-c), indicating significant internalization. In contrast, cells treated with free CPT showed no observable fluorescence, as indicated in Figure 4.

The MTT assay results exhibited that the CPT-loaded SPION@DEX-FA nanoparticles caused a significant, dose-dependent decrease in the viability of prostate cancer cells. In contrast, free CPT and the bare SPION@DEX-FA nanocarrier did not display significant cytotoxicity, with over 90% of cells remaining viable after 48 hours. The CPT-loaded construction showed minimal toxicity near normal prostate cells. The IC50 values against cancer cells were 12 µg/mL at 24 hours and 20 µg/mL at 48 hours (Figure 5a and 5-b).

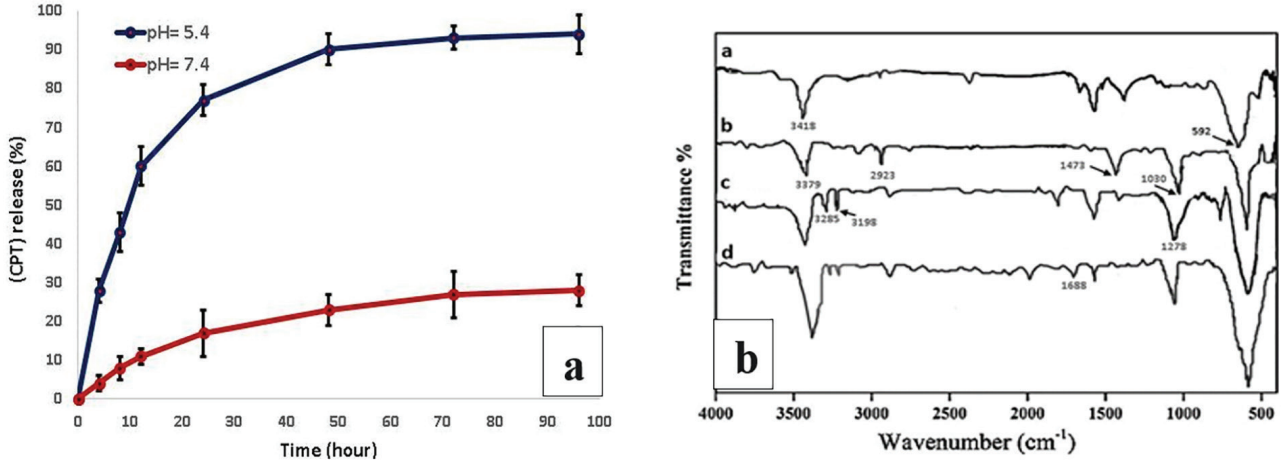

Figure 3: a: Camptothecin (CPT) release profile from supermagnetic iron oxide-dextran-camptothecin-folic acid nanoparticles (SPION-DEX-CPT-FA) nanoparticles at different pH values over 96 hours. b**:** Fourier Transform Infrared (FTIR) spectra of (a) supermagnetic iron oxide nanoparticles (SPIONs), (b) supermagnetic iron oxide-dextran (SPION-DEX), (c) supermagnetic iron oxide-dextran (SPION-DEX-CPT), (d) SPION-DEX-CPT-FA–FA.

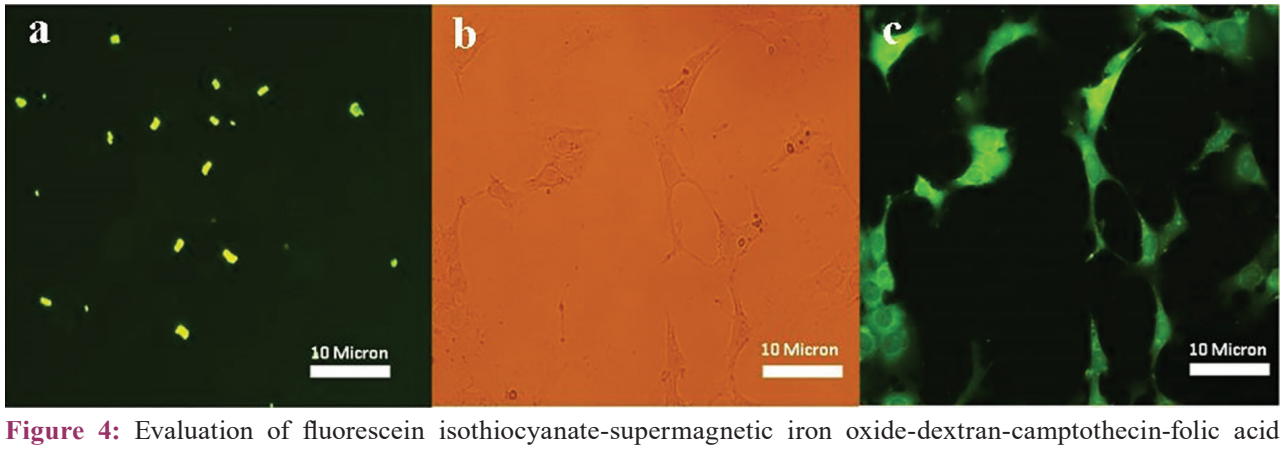

Figure 4: Evaluation of fluorescein isothiocyanate-supermagnetic iron oxide-dextran-camptothecin-folic acid nanoparticles (FITC-SPION-DEX-CPT-FA) uptake by fluorescence imaging in prostate cancer cells (400x magnification). (a) Fluorescence micrograph of camptothecin (CPT)-treated cells. (b) Optical micrograph of FITC-SPION-DEX-CPT-FA-treated cells. (c) Fluorescence image of FITC-SPION-DEX-CPT-FA-treated cells.

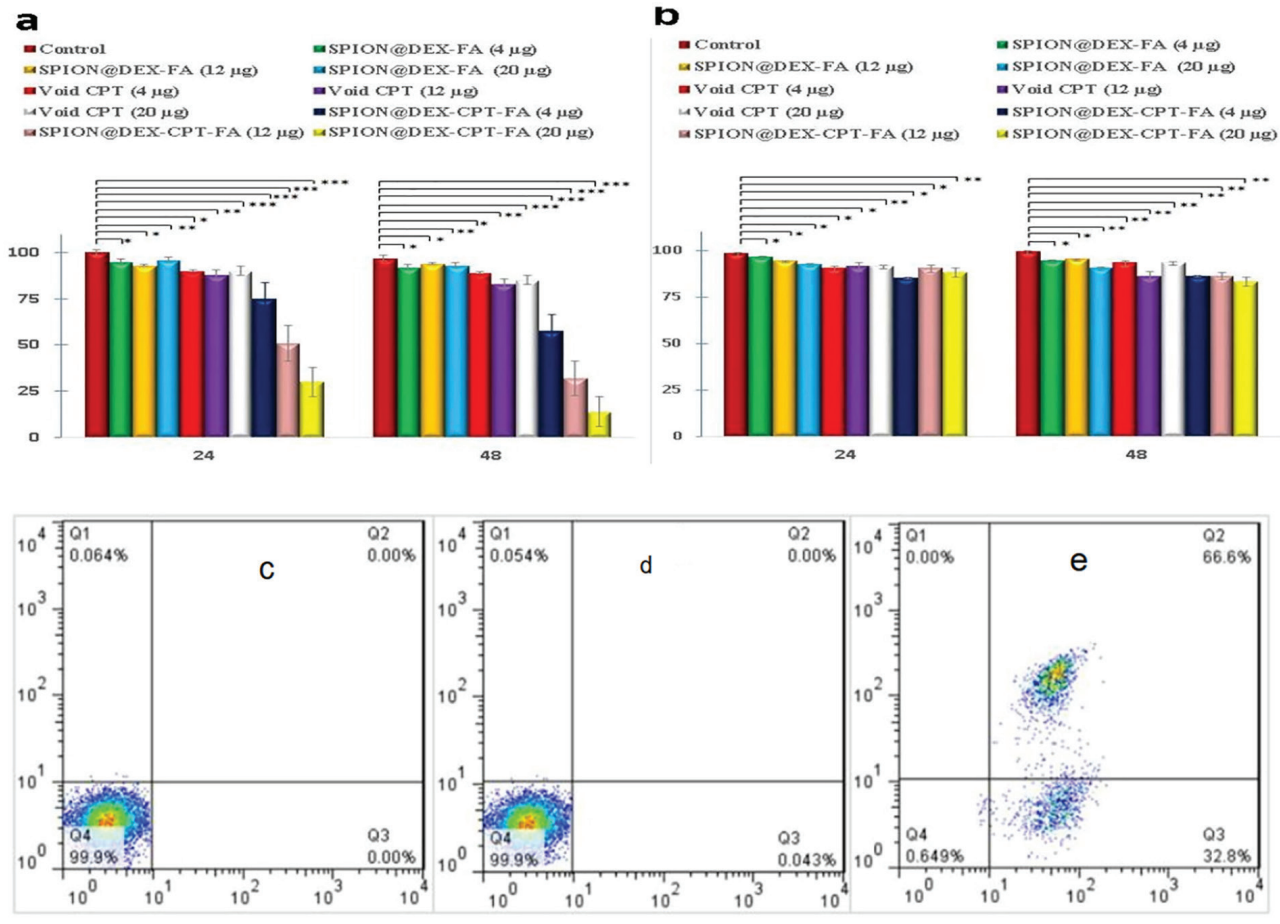

Figure 5: MTT assay results showing the cytotoxicity of different formulations on prostate cancer and normal cells. Induction of apoptosis by the supermagnetic iron oxide-dextran-camptothecin-folic acid nanoparticles (SPION-DEX-CPT-FA) nanocarrier. Cell lines were treated with (c) empty camptothecin (CPT), (d) SPION@DEX-FA, and (e) SPION@DEX-CPT-FA.

Flow cytometry analysis after 48 hours of treatment showed that the SPION@DEX-CPT-FA nanoformulation (e) induced a marked increase in the apoptotic cell population in prostate cancer cells. Treatment with empty CPT (c) and the bare SPION@DEX-FA nanocarrier (d) resulted in minimal apoptotic effects (Figure 5).

Discussion

This study successfully developed a multifunctional nanocomposite of SPION@DEX-CPT-FA, to target *in vitro* cancer therapy. The physicochemical characterization established the rational design of the raised area. The significant increase in hydrodynamic diameter as from 17.21 nm for the naked SPIONs to 64.38 nm for the final composite, provided solid evidence of the successful sequential coating through dextran, CPT, and folic acid. The finding is consistent with a previous report on surface-modified nanoparticles (22). The greatly negative zeta potential of -43.8 mV indicated an excellent colloidal stability, which is precarious for preventing accumulation in the bloodstream. This stability is attributed to sturdy electrostatic repulsion between elements, that further was enhanced by the steric interruption provided by the hydrophilic dextran polymer shell (19, 23-25).

The FTIR analysis provided decisive chemical proof of the nanocomposite's structure. The appearance of characteristic peaks for each component at separate stages of synthesis confirmed the successful coating of dextran, encapsulation of CPT, and, most prominently, the conjugation of FA. The VSM outcomes showed an expected reduction in overload magnetization after coating, as the non-magnetic organic coats contribute to the total mass. However, the retained value of 19.7 emu/g is sufficient for likely applications in magnetic targeting or MRI, while the preservation of superparamagnetic actions ensures the particles will not totally magnetize after the external field is impassive.(15, 26, 27).

The functional performance of the nanocomposite was correspondingly impressive. The high encapsulation efficiency of 64.38% highlights the crucial role of the dextran matrix in effectively charging the hydrophobic CPT (28). The pH-responsive medicine release is a key aspect of this "smart" delivery system. The gentle release at

physiological pH (7.4) minimizes previous drug leakage in circulation, while the accelerated release at acidic pH (5.4) ensures that the therapeutic payload is preferentially distributed within the acidic microenvironment of tumors or exclusive endo-lysosomal compartments following cellular uptake, while also incorporating blood pressure in versus breeds (29-31).

It seems that MRI both *in vitro* and *in vivo* can determine the fate of various cells when labeled with SPIONs that can affect the outcome of treatment (32-35). The biological evaluations confirmed the targeting strategy. The powerful fluorescence observed in cancer cells frozen with the nanocomposite proved that the FA ligand effectively mediated cellular uptake by folate receptor-mediated endocytosis. (3, 36). This targeted internalization directly transforms into enhanced and selective cytotoxicity. The low IC50 value against prostate cancer cells, fixed with the negligible effect on normal cells, demonstrated the platform's capacity to distinguish between malignant and healthy tissue. The primary mechanism of cell death was confirmed to be apoptosis, a controlled also non-inflammatory pathway that is highly desirable in cancer therapy (37). The synergistic effect of the targeted delivery system was evident, as neither the free drug nor the empty carrier alone could induce substantial apoptosis. (22, 38).

Conclusion

This study revealed the positive synthesis and comprehensive evaluation of a folic acid-targeted, pH-responsive, superparamagnetic nanocomposite (SPION@DEX-CPT-FA) for the transfer of camptothecin. The well-characterized platform confirmed excellent colloidal stability, high drug charging capacity, and intelligent, pH-triggered drug release. *In vitro* studies established the nanocomposite to be selectively internalized via prostate cancer cells, leading to potent and specific cytotoxicity through the induction of apoptosis, while sparing normal cells. These findings suggest that the SPION@DEX-CPT-FA system is a greatly promising nanocarrier for battered cancer therapy, warranting further examination in preclinical *in vivo* models.

Acknowledgement

We would like to gratitude Biotechnology Medical Department, College of Biotechnology, Al-Qasim Green University for supporting this research work.

Funding

No funds received for this study.

Authors' Contribution

Qasim designed the study and significantly contributed with Sharafaldin to review the article, Mosaab gathering the samples, contributed data analysis and prepared the first version of the manuscript writing and editing of the final version.

Conflict of Interest

None declared.

References

1 Kratzer TB, Mazzitelli N, Star J, Dahut WL, Jemal A, Siegel RL. Prostate cancer statistics, 2025. CA Cancer J Clin. 2025;75:485-497. DOI: 10.3322/caac.70028. PMID: 40892160.

2 Farahmand M, Khademolhosseini F, Mehrabani D. Trend Of Prostate Cancer In Fars Province, Southern Iran, 2001-2007. *J Res Med Sci*. 2010;15:295-7. PMID: 21526101.

3 Pourmasoumi P, Banihashemian SA, Zamani F, et al. Nanoparticle-Based Approaches in the Diagnosis and Treatment of Brain Tumors. *J Clin Med*. 2024;13:7449. DOI: 10.3390/jcm13237449. PMID: 39685907.

4 Zare S, Mehrabani D, Jalli R, et al. MRI-Tracking of Dental Pulp Stem Cells In Vitro and In Vivo Using Dextran-Coated Superparamagnetic Iron Oxide Nanoparticles. *J Clin Med.* 2019;8:1418. DOI: 10.3390/jcm8091418. PMID: 31505807.

5 Horvat NK, Chocarro S, Marques O, et al. Superparamagnetic iron oxide nanoparticles reprogram the tumor microenvironment and reduce lung cancer regrowth after crizotinib treatment. *ACS Nano*. 2024;18:11025-41. DOI: 10.1021/acsnano.3c08335. PMID: 38626916.

6 Abed DA, Hamzah KJ, Abdul-kareem S, et al. Bacteriological and molecular study of some urinary tract infections bacteria in human and cows in Babylon Province. *Pak Vet J*. 2024;44: 1249-1254. DOI: 10.29261/pakvetj/2024.285.

7 Panda J, Satapathy BS, Mishra A, et al. Potential of ferrite-based nanoparticles for improved cancer therapy: recent progress and challenges ahead. Applications of Ferrites. 2023. DOI: 10.5772/intechopen.1002346.

8 Jalli R, Mehrabani D, Zare S, et al. Cell Proliferation, Viability, Differentiation, and Apoptosis of Iron Oxide Labeled Stem Cells Transfected with Lipofectamine Assessed by MRI. *J Clin Med*. 2023;12:2395. DOI: 10.3390/jcm12062395. PMID: 36983399.

9 Al-Mousawi HM, Jadooa MM, Al-Bderee NM. Effectiveness of green synthesized ZnO nanoparticles against MDR Klebsiella pneumoniae isolated from diabetic foot. *Indones*

J Health Sci Med. 2024;1:57-10. DOI:10.21070/ijhsm.v2i1.57.

10 Pérez-Ortega HU, Córdova-Espíritu RR, Cano-Serrano S, et al. Camptothecin in cancer therapy: current challenges and emerging strategies with nanoemulsions. *Pharmaceutics*. 2025;17:1414. DOI: 10.3390/pharmaceutics17111414. PMID: 41304752.

11 Kizisar D, Subasi NT, Eroksuz S, et al. Investigation of the stabilization of camptothecin anticancer drug via PSA-PEG polymeric particles. *Anadolu Univ J Sci Technol A*. 2016;17:221-31. DOI:10.18038/btda.87862.

12 Malhotra S, Dumoga S, Joshi A, et al. Polymeric micelles coated with hybrid nanovesicles enhance the therapeutic potential of camptothecin. *Acta Biomater*. 2021;121:579-91. DOI: 10.1016/j.actbio.2020.11.049. PMID: 33285325.

13 Alnasraui AHF, Joe IH, Al-Musawi S. Design and synthesis of folate-decorated Fe3O4@Au-DEX-CP nanoformulation for targeted drug delivery in colorectal cancer therapy: in vitro and in vivo studies. *J Drug Deliv Sci Technol*. 2023;87:104798. DOI: 10.1016/j.jddst.2023.104798.

14 Hashemi SS, Niknam Z, Mojtaba Zebarjad S, et al. Tracking the healing effect of human Wharton's jelly stem cells labeled with superparamagnetic iron oxide nanoparticles seeded onto polyvinyl alcohol/chitosan/carbon nanotubes in burn wounds by MRI and Prussian blue staining. *Biomed Mater*. 2025;20. DOI: 10.1088/1748-605X/ad9fc6. PMID: 39681069.

15 Mehrabani D, Nazempour M, Mehdinavaz-Aghdam R, et al. MRI tracking of human Wharton's jelly stem cells seeded onto acellular dermal matrix labeled with superparamagnetic iron oxide nanoparticles in burn wounds. *Burns Trauma*. 2022;10:tkac018. DOI: 10.1093/burnst/tkac018. PMID: 36380853.

16 Iravani K, Mehrabani D, Doostkam A, et al. Use of Magnetic Resonance Imaging to Assess the Regenerative Effects of Adipose Tissue-Derived Mesenchymal Stem Cells in a Rabbit Cartilaginous Laryngeal Defect Model. *Curr Ther Res Clin Exp*. 2022;97:100682. DOI: 10.1016/j.curtheres.2022.100682. PMID: 35959231.

17 Vegrim HM, Dreier JW, Igland J, et al. High-dose folic acid use and cancer risk in women who have given birth. *Epilepsia*. 2025;66:75-88. DOI: 10.1111/epi.18146. PMID: 39540679.

18 Cheung A, Bax HJ, Josephs DH, et al. Targeting folate receptor alpha for cancer treatment. *Oncotarget*. 2016;7:52553. DOI: 10.18632/oncotarget.9651. PMID: 27248175.

19 Wasiak I, Kulikowska A, Janczewska M, et al. Dextran nanoparticle synthesis and properties. *PLoS One*. 2016;11:e0146237. DOI: 10.1371/journal.pone.0146237. PMID: 26752182.

20 Mahdi SA, Kadhim AA, Albukhaty S, et al. Gene expression and apoptosis in hepatocellular carcinoma cells induced by polymer/magnetic nanoparticles containing 5-fluorouracil. *Electron J Biotechnol*. 2021;52:21-9. DOI: 10.1016/j.ejbt.2021.04.001.

21 Al-Murrani, Waleed. General, biological and biomedical statistics. Cambridge Scholars Publishing, 2024.

22 Sadighian S, Rostamizadeh K, Hosseini-Monfared H, et al. Doxorubicin-conjugated core–shell magnetite nanoparticles for anticancer drug delivery. Colloids Surf B Biointerfaces. 2014;117:406-13. DOI: 10.1016/j.colsurfb.2014.03.001. PMID: 24675279.

23 Du H, Bai J, Zuo C, et al. Hierarchical supra-nanostructure of HKUST-1 featuring enhanced H2 adsorption enthalpy and higher mesoporosity. *CrystEngComm*. 2011;13:3314-6.

24 Alnasraui AHF, Al-Musawi S, editors. Nanoformulation of intelligent polymeric nanocarrier for resveratrol targeted delivery: cytotoxic, apoptotic, and genetic effects. AIP Conf Proc. 2022.

25 Moghaddam A, Sadeghinia A, Saebi Y, et al. Electrochemical Interfaces Enhanced by Silver Nanoparticles: Insights from Biosensing Research. *J Electrochem Soc*. 2025;172:087505. DOI: 10.1149/1945-7111/adf46c.

26 Ahmad T, Wani IA, Manzoor N, et al. Biosynthesis and antimicrobial activity of gold and silver nanoparticles. *Colloids Surf B Biointerfaces*. 2013;107:227-34. DOI: 10.1016/j.colsurfb.2013.02.004. PMID: 23500733.

27 Al-Bderee NMH, Al-Janabi N, Al-Saad NFN, et al. Enterobacter cloacae lipopolysaccharide export system protein (LptC) gene expression after exposure to biosynthesized ZnO nanoparticles. *J Microbiol Biotechnol Food Sci*. 2024;14:e10785. DOI: 10.55251/jmbfs.10785.

28 Ghaferi M, Asadollahzadeh MJ, Akbarzadeh A, et al. Enhanced efficacy of PEGylated liposomal cisplatin. *Int J Mol Sci*. 2020;21:559. DOI: 10.3390/ijms21020559. PMID: 31952316.

29 Hamzah KJ, Mahmood AK, Saad MH. Comparative study of blood pressure between local and foreign dog breeds in Iraq. *Biochem Cell Arch*. 2019;19:2853. DOI: 10.35124/bca.2019.19.2.2853.

30 Albukhaty S, Al-Musawi S, Abdul Mahdi S, et al. Dextran-coated superparamagnetic

nanoparticles for vinblastine controlled release and gene expression in pancreatic cancer cells. *Molecules*. 2020;25:4721. DOI: 10.3390/molecules25204721. PMID: 33076247.

31 Jalehrokhnezhad M, Malakootikhah J. Nano-encapsulation of medicinal plant extracts in Iran (2019–2024): techniques and antimicrobial applications. *J Med Bacteriol*. 2025:118-30. DOI: 10.18502/jmb.v13i3.19515.

32 Bozorg-Ghalati F, Hedayati M, Dianatpour M, et al. Effects of a phosphoinositide-3-kinase inhibitor on anaplastic thyroid cancer stem cells. *Asian Pac J Cancer Prev*. 2017;18:2287-2291. DOI: 10.22034/APJCP.2017.18.8.2287. PMID: 28843268.

33 Shamsnia SJ, Khezri AA, Tabbatabaei HR, et al. Survival from bladder cancer in shiraz, southern iran: a hospital-based study. *Middle East J Sci Res*. 2013;18:425-31. DOI: 10.5829/idosi.mejsr.2013.18.4.7542.

34 Farahmand M, Khademolhosseini F, Medhati M, et al. Trend Of Bladder Cancer In Fars Province, Southern Iran, 2002-2006. *Iran Red Crescent Med J*. 2009;11:5-8.

35 Mehrabani D, Tabei SZ, Heydari ST, et al. Cancer Occurrence In Fars Province, Southern Iran. *Iran Red Crescent Med J*. 2008;10:314-22.

36 Farhan MM, Hashim NM. Glucosinolate hydrolysis products from broccoli altering VEGF and HUR expression in A549 cells. *Turk J Physiother Rehabil*. 32:4012-4020.

37 Abroudi M, Mehrabani D, Zare S, et al. In Vitro Assessment of Morphology, Proliferation, Apoptosis and Differential Potential of Dental Pulp Stem Cells, When Marijuana Is Added to Nutrients of Cell Culture Medium. *Int J Nutr Sci*. 2024;9:62-70. DOI: 10.30476/IJNS.2024.101034.1288.

38 Al-Musawi S, Hadi AJ, Hadi SJ, et al. Folated chitosan–magnetic nanocarrier for 5-fluorouracil delivery in bladder cancer therapy. *J Glob Pharm Technol*. 2019;11:628-37.